

## Synthesis of Nanocrystalline Titanium Diboride in a Hypervelocity Plasma Jet

A. A. Sivkov, D. Yu. Gerasimov, and D. S. Nikitin\*

Tomsk Polytechnic University, Tomsk, 634050 Russia

\*e-mail: NikitinDmSr@yandex.ru

Received September 15, 2017

**Abstract**—Results of experimental investigations of directly synthesizing nanocrystalline titanium diboride in a hypervelocity jet of electrodischarge plasma generated by a pulse high-current coaxial magnetoplasma accelerator with titanium electrodes are presented. The main result of the investigations is manufacturing a product with a mass of up to ~3 g containing more than 90% of titanium diboride obtained mostly in the form of hexagonal and dodecagonal particles.

DOI: 10.1134/S1063785018040090

At present, creating materials with high physicomechanical and thermal characteristics for further use in various branches of industry, in particular, the aerospace, arms, and automobile industries, is highly topical. Titanium diboride is such a material in view of its high values of hardness, elasticity modulus, melting temperature, and resistance to high-temperature oxidation.  $\text{TiB}_2$  does not enter into reactions with molten steel, cast iron, zinc, and many other metals [1–3]. Such properties allow one to use titanium diboride as a basis for creating thermocouples and their protective coatings, elements of metallurgical furnaces and electrolysis units, high-temperature alloys, instrument and abrasive materials, details of jet-propulsion units and turbines, wear-resistant ceramics, and coatings of different purpose [4–6]. The scientific community is also greatly interested in titanium diboride in the nanosize state: addition of  $\text{TiB}_2$  nanoparticles to metal-based composites allows one to improve the hardness of the final product [7], nanostructured  $\text{TiB}_2$ -based ceramics exhibit higher fracture toughness, plasticity, and ease of packing as compared to a macrosized product [8]. Nanosize titanium diboride can be synthesized using different technologies, including mechanical synthesis, self-propagating high-temperature synthesis, and the sol-gel method [9]. However, most methods of  $\text{TiB}_2$  synthesis are fraught with difficulties in implementing the processes, expensiveness of precursors, and unsatisfactory quality of the product [10].

A promising way to synthesize nanosize particles and nanostructured coatings is the plasmadynamic method, which is based on using a hypervelocity plasma jet generated by a pulse ( $t \sim 300 \mu\text{s}$ ) high-current ( $I \sim 100 \text{ kA}$ ) coaxial magnetoplasma accelerator

(CMPA). The principle of operation of this electrical device, which is classified as a  $Z$ -pinch accelerator, lies in the appearance of a plasma bridge in the gap between the central electrode and barrel electrode, as well as in the further compression, confinement, and acceleration of the obtained plasma flow due to ponderomotive force  $F$  of the interaction between magnetic field  $B$  inside the barrel electrode and current  $I$  generating it. In the bow shock wave of a plasma flow accelerated to supersonic velocities, extreme energetic parameters (high pressure and temperature) are generated. Given these parameters, according to the diagram of states, the phase synthesis of titanium boride and diboride occurs in the liquid state and, then, nanoparticles are formed under conditions of quenching. Thus, the aim of this work is to implement the plasmadynamic synthesis of a powdered product with a high phase output of nanocrystalline titanium diboride.

This work involves a CMPA with titanium electrodes [11]. Titanium eroded from the surface of the acceleration channel and boron embedded in the plasma-structure-formation channel (PSFC) between the central and barrel electrodes served as precursors of the chemical reaction. The CMPA was supplied with electric power using a capacitive-energy storage with a capacitor bank of  $C = 6 \text{ mF}$  and charging voltage of  $U = 3.0 \text{ kV}$ . The energy released in the experimental process was  $W = 37 \text{ kJ}$ .

Since boron embedded in a plasma-structure-formation channel is a semiconductor material, it was necessary to use additional means to bring about the plasma jet. In this work, it was initiated by PSFC graphitization: a thin layer of graphite aerosol was deposited on the inner PSFC surface. Plasma-jet ini-

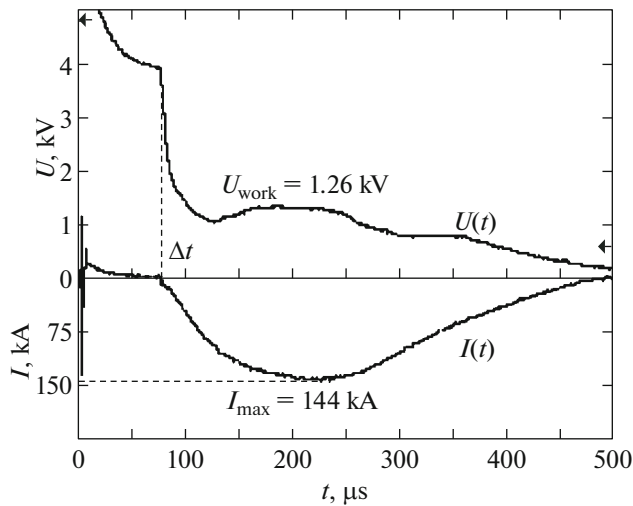


Fig. 1. Waveforms of current  $I(t)$  and voltage  $U(t)$  in the experimental process.

tiation by graphitization significantly distinguishes this investigation from that carried out in [12] where the jet was initiated by using thin titanium and copper wires tightened over the inner PSFC surface and connecting the central and barrel electrodes. The primary problem of obtaining the product with a predominant content of titanium diboride was not solved. The main consequence of the change in the way of initiating the plasma jet is the change in the character of waveforms of the current  $I(t)$  and voltage  $U(t)$  (the waveforms are presented in Fig. 1). Using wires leads to the appearance of a sharp initial process ( $\Delta t = 20 \mu\text{s}$ ) and to the presence of a typical voltage pulse, which is explained by the electric explosion of the titanium or copper conductors; in the case of PSFC graphitization, there

is a long preliminary delay stage ( $\Delta t = 80 \mu\text{s}$ ) and the voltage pulse is absent. In the latter case, the precursor introduced into the PSFC is heated during the delay time and, since the process runs more smoothly and slowly, boron is introduced into the reaction zone most completely.

The experiment resulted in obtaining a sample of a powdered product with a mass of  $\sim 3 \text{ g}$  (in a single experimental cycle). Then, the sample was investigated without preliminary preparations by different methods. First of all, the product was analyzed by methods of X-ray diffractometry. Using a Shimadzu XRD-7000 X-ray diffractometer ( $\text{CuK}\alpha$  radiation), a product diffractogram depicted in Fig. 2 was obtained. The diffractogram includes a collection of intensity maximums corresponding to two crystalline phases:  $\text{TiB}_2$  (ICDD Card No. 00-07-0275; hexagonal, space group  $P6/mmm$  N 191) and  $\text{TiB}$  (ICDD Card No. 00-06-0641; cubic, space group  $Fm\bar{3}m$  N 225).

Quantitative analysis of the phase composition of the product was carried out by calculations using the PowderCell 2.0 software based on the Rietveld method, with the use of the PDF4+ database. Results of the quantitative analysis are presented in Table 1. The calculation Q-factor ( $R_{wp}/R_{exp}$ )<sup>2</sup> testifies to the correctness of results from [13]. It is seen from the table that the product contains mostly the phase of hexagonal titanium diboride  $\text{TiB}_2$  (93.2%). In addition, there is the phase of titanium boride with a content of 6.8%. Comparison with results of [12] shows a significant difference in the  $\text{TiB}_2$  content, which is not merely evidence of the possibility in principle of synthesizing nanosize  $\text{TiB}_2$  particles in a hypervelocity plasma jet, but also testifies that a high-purity nano-

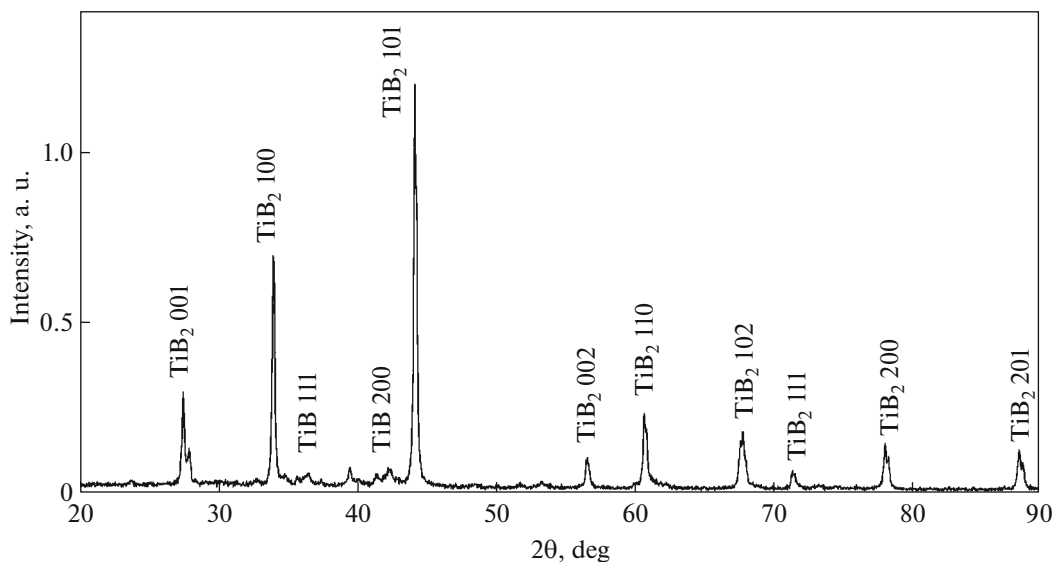


Fig. 2. X-ray diffractogram of the synthesized powdered product.

dispersed titanium-diboride powder has been obtained.

Coherent scattering regions (CSRs) were calculated using the Debye–Scherrer formula. The CSR indirectly indicates the average particle size in the product. According to values of the CSR size, the main fraction of particles of all crystalline phases is nanosize; at the same time, the CSR value for titanium diboride considerably exceeds the same value for titanium boride, which points to a noticeable difference in the dimensions of particles for these phases.

The microstructure of the powdered synthesis product was studied by means of transmission electron microscopy using a Philips CM 12 microscope. Figure 3a shows a bright-field micrograph in which a typical aggregate of synthesis-product particles is seen. The overwhelming majority of particles are polyhedrons whose projections onto the image plane are close to circles with dimensions of up to 140 nm. On the basis of a collection of available micrographs (a sample of 1000 objects), the particle size was analyzed and the histogram of the particle-size distribution was constructed (Fig. 3b). A pronounced maximum is seen in the histogram at 40 nm, with the calculated value of the average particle size being  $d_{av} = 49$  nm, which is close to the CSR value calculated for the  $TiB_2$  phase. This suggests that the overwhelming majority of crystalline objects visible in the micrograph belong to the titanium-diboride phase.

Figure 3c presents the electron-diffraction pattern on a distinguished region of the aforementioned aggregate. This is a collection of point reflexes which predominantly correspond to interplanar distances for

**Table 1.** Main data of the full-profile phase-structure analysis of the synthesized product (content  $\omega$  and CSR size  $d$ )

Parameter	$TiB_2$	TiB	$(R_{wp}/R_{exp})^2$
$\omega$ , mass %	93.2	6.8	1.51
$d$ , nm	50	17	

the titanium-diboride phase. Figure 3d shows a dark-field image obtained in  $TiB_2$  (101) reflexes. In this image, objects are distinguished in the form of prisms with hexagonal (objects 1 in the bright- and dark-field micrographs) and dodecagonal (objects 2) bases—typical hexagonal and dodecagonal particles corresponding to simple figures for the spatial group of titanium diboride and shape of Wulff crystals.

Thus, this work presents the results of experimental studies of synthesis in the titanium–boron system in a hypervelocity plasma jet generated by a coaxial magnetoplasma accelerator. The main result of the work is the obtaining of a powdered product with a mass of  $\sim 3$  g (in a single experimental cycle). According to the study of this product by several analytical techniques, it consists mostly (more than 90%) of the crystalline phase of titanium diboride  $TiB_2$  in the form of nanosize hexagonal and dodecagonal particles.

**Acknowledgments.** This work was supported by the Russian Science Foundation (project no. 15-19-00049) and Competitiveness Program of Tomsk Polytechnic University.

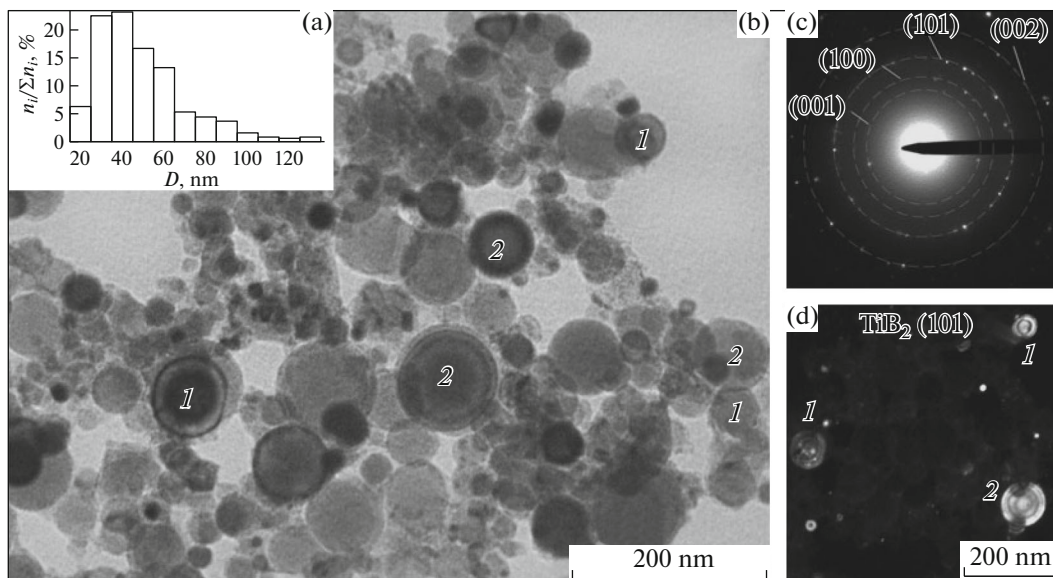


**Fig. 3.** Results of studying the synthesis product by methods of transmission electron microscopy: (a) bright-field micrograph of an aggregate of particles, (b) histogram of the product particle-size distribution, (c) electron-diffraction pattern of the corresponding aggregate of particles, and (d) dark-field micrograph of an aggregate of particles in light of the  $TiB_2$  (101) reflex.

## REFERENCES

1. R. A. Andrievskii, *Usp. Khim.* **84**, 540 (2015).
2. W. G. Fahrenholtz, E. J. Wuchina, W. E. Lee, and Y. Zhou, *Ultra-High Temperature Ceramics: Materials for Extreme Environment Applications* (Wiley, Hoboken, NJ, 2011).
3. H. Xiang, Z. Feng, Z. Li, and Y. Zhou, *J. Appl. Phys.* **117**, 225902 (2015).
4. Y. Shen, X. Li, T. Hong, J. Geng, and H. Wang, *Mater. Sci. Eng., A* **655**, 265 (2016).
5. S. Carenco, D. Portehault, C. Boissière, N. Mézailles, and C. Sanchez, *Chem. Rev.* **113**, 7981 (2013).
6. J. Tang, *Appl. Surf. Sci.* **365**, 202 (2016).
7. S. Klébert, A. M. Keszler, I. Sajó, E. Drotár, I. Bertóti, E. Bodis, P. Fazekas, Z. Károly, and J. Szépvölgyi, *Ceram. Int.* **40**, 3925 (2014).
8. D. Demirskyi, D. Agrawal, and A. Ragulya, *Ceram. Int.* **40**, 1303 (2014).
9. A. Nozari, S. Heshmati-Manesh, and A. Ataie, *Int. J. Refract. Met. Hard Mater.* **33**, 107 (2012).
10. K. Bao, Y. Wen, M. Khangkhamano, and S. Zhang, *J. Am. Ceram. Soc.* **100**, 2266 (2017).
11. A. A. Sivkov, D. Yu. Gerasimov, and D. S. Nikitin, *Tech. Phys. Lett.* **43**, 16 (2017).
12. D. Nikitin, A. Sivkov, D. Gerasimov, and A. Evdokimov, in *Proceedings of the 11th International Forum on Strategic Technology (IFOST-2016), Novosibirsk, 2016*, p. 170.
13. A. K. Tripathi, M. C. Mathpal, P. Kumar, M. K. Singh, S. K. Mishra, R. K. Srivastava, J. S. Chung, G. Verma, M. M. Ahmad, and A. Agarwal, *Mater. Sci. Semicond. Process.* **23**, 136 (2014).

*Translated by A. Nikol'skii*